Talanta 86 (2011) 421–424

Contents lists available at SciVerse ScienceDirect

Talanta

journal homepage: www.elsevier.com/locate/talanta

Short communication

Reflection spectroscopy for the determination of Au nanostructure formation on carbon surfaces

Xin Ran Cheng, Anthony J. Veloso, Kagan Kerman*

Department of Physical and Environmental Sciences, University of Toronto Scarborough, 1265 Military Trail, M1C 1A4 Toronto, ON, Canada

ARTICLE INFO

Article history:
Received 27 October 2010
Received in revised form 21 August 2011
Accepted 22 August 2011
Available online 26 August 2011

Keywords:
Electrodeposition
Reflectance spectroscopy
Screen-printed chips
Au nanostructures

ABSTRACT

Au electrodeposition has been performed on carbon electrodes to fabricate Au nanostructures on the working electrode of screen-printed carbon chips. The amount of Au deposited was characterized using the raw reflection spectra obtained by detecting UV–Vis spectrum reflected from the electrode surface. SEM images at different deposition time points provided evidence for the growth of Au nanostructures. The increase in deposition time led to an increase in the intensity of the spectrum obtained for both chips. The acquired optical properties of the carbon chips provide a promising platform for simultaneous optical and electrochemical measurements.

1. Introduction

The deposition of metallic thin films has always been intriguing to material scientists and surface physicists. The electrodeposition of Au nanostructures on electrode surfaces has been suggested as an attractive process to increase the electrode conductivity, facilitating electron transfer and improving its sensitivity [1]. The detection of Au electrodeposition with optical characterization enables fast examination of the surface.

The morphology of electrodeposited Au nanostructures has been well characterized. Ohsaka and coworkers have reported electrodeposition of Au nanostructures and nanostructures with unique shapes, such as floral, thorny and dendritic morphology on carbon and Au electrodes [2]. Sakai and coworkers [3] had characterized the electrodeposition of Au nanostructures on indium tin oxide substrates and found similar structures in their deposited Au using atomic force microscopy. Scanning electron micrographs suggest that Au electrodeposition occurs by instantaneous nucleation before they grow into three-dimensional semispherical particles [4]. Electrochemical deposition of Au on surfaces is convenient and fast. It also exhibits control over the thickness of the Au layer by varying the time of deposition and the voltage applied. In order to apply biosensors widely, it is necessary to develop cost effective, disposable, highly sensitive and reproducible devices. Screen printing has become a powerful technique that can produce almost identical copies of electrodes [1]. Electrodeposition of metal nanostructures onto screen-printed electrodes has various application possibilities like detection of hydrazine on Pd-plated boron doped diamond microdisc array [5], electrochemical reduction of oxygen on Au nanostructures [6] and measurement of polyphenol in wine [7]. Because of these wide application possibilities, it is advantageous to develop a cost effective, disposable, highly sensitive and reproducible device. These chips may then promise the mass production of electrochemical biosensors possessing various catalytic activities [1]. Combining the potential of generating a more sensitive electrode by electrodeposition of Au and the cost effectiveness of screen-printed carbon electrodes, it is theoretically possible to make a powerful and affordable biomedical tool. With this combination, both electrochemical and optical properties could be measured. Such electrochemical localized surface plasmon resonance (E-LSPR) provided a highly sensitive and reliable complementary analysis of bimolecular interactions [8]. However, often the fabrication of the membranes for Au films requires tedious steps before any optical or electrochemical measurements could be performed [9–14].

In this communication, the optical properties (raw reflection spectra in scope mode) of the two different types of screen-printed chips were measured directly before and after electrodeposition of the Au nanostructures. The results were supported by scanning electron microscope (SEM) images.

2. Experimental

2.1. Reagents and apparatus

Stock solutions of $HAuCl_4 \cdot 3H_2O$, 99.99+% (Sigma–Aldrich) were prepared in 0.1 M HCl (pH 1.2). Electrodeposition of Au was

* Corresponding author. Tel.: +1 416 287 7250; fax: +1 416 7279.
E-mail address: kagan.kerman@utoronto.ca (K. Kerman).

0039-9140/$ – see front matter © 2011 Elsevier B.V. All rights reserved.
doi:10.1016/j.talanta.2011.08.039

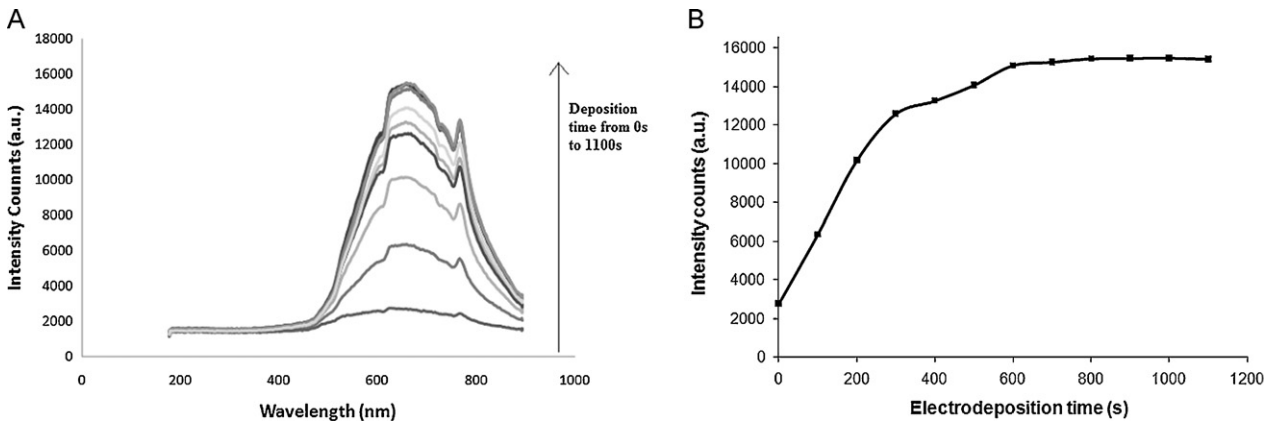

Fig. 1. Optical characterization of SPCE chips after electrodeposition. (A) Raw reflection spectra taken in scope mode of the working electrode area of the Au deposited chips with increasing intensities from deposition times of 0 s to 1100 s. (B) Deposition time dependence of peak intensity of raw reflection spectra at 658 nm.

performed using CHI400A electrochemical analyzer (CH Instruments Inc., Austin, USA). The disposable electrochemically printed chips (DEP-ER-N) were donated by Professor Eiichi Tamiya (Osaka University, Japan) and Biodevice Technology Ltd. (Kanazawa, Japan). These screen-printed carbon electrode (SPCE) chips also comprised of a three-electrode system with a working electrode (2.64 mm^2 area), a carbon counter electrode and Ag/AgCl reference electrode.

2.2. Electrodeposition of Au nanostructures

The electrodeposition of Au nanostructures was performed in 40 μL of the corresponding concentrations (1 mM for SPCE chips) of $HAuCl_4$ solution covering all three electrodes while applying a potential of −0.4 V for different periods of time [1]. The raw reflection values at various wavelengths were measured and plotted on a graph. All measurements were carried out at room temperature ($23 \pm 2\,^{\circ}C$).

The electrodes were blotted and left to fully dry in a fume hood (semi-covered in petri dish) after electrodeposition. The electrodes' reflection spectra were measured using an optics system that was composed of a spectrophotometer (USB-4000-UV-Vis), a tungsten halogen light source (LS-1-LL, wavelength range 200–1100 nm) and a fiber probe bundle (fiber core diameter 400 μm, wavelength range 300–1100 nm), all purchased from Ocean Optics (Dunedin, USA). The UV–Vis probe was placed close to the working electrode surface so that incident light was reflected upon hitting the surface and then backed in the detector situated in the light probe. The Scope Processing Mode of the Spectra Suite software was used to measure the spectral characteristics of the samples.

Impedance electrochemical spectroscopy and cyclic voltammetry were performed with μAutolab-III electrochemical analysis system (Metrohm, Switzerland). Impedance measurements were taken over the range of frequencies from 100 kHz to 100 MHz, with 5 mV as the amplitude at an applied polarization potential of the maxima of the chip's cyclic voltammetry scan using 20 mM $[Fe(CN)_6]^{(4-/3-)}$ (1:1 molar ratio) in PBS buffer containing 100 mM NaCl. This was used in conjunction with its frequency response analyzer (FRA) system (Metrohm, Switzerland). Cyclic voltammetry was also performed with μAutolab-III electrochemical analyzer as well, but operated in conjunction with its general purpose electrochemistry software (GPES) instead.

LEO (Zeiss) 1530 scanning electron microscope was used (University of Western Ontario, Canada) at an acceleration voltage of 3.00 kV and at a vacuum pressure of 2×10^{-6} Mbar. The images were taken with the SPCE chips mounted on the metal specimen table with copper tape.

3. Results and discussion

Applying a negative potential across the carbon electrodes enabled the formation of a layer as the Au cations in the solution were reduced to Au^0. The Au nanostructures deposited had a higher reflectivity than the carbon working electrodes. Therefore, a higher intensity of reflection was observed when UV–Vis light was exposed on the chips. The raw reflection spectrum of the Au electrodeposition was plotted from 0 s to 1100 s and an increasing trend was observed between peak intensities and the duration of electrodeposition (Fig. 1A). An electrodeposition time dependence curve of the peak reflection intensity at 658 nm (Fig. 1B) showed that the saturation point of Au deposition occurred at about 600 s with the 10 mM $HAuCl_4$ solution. This was probably because most of the cations in the 40 μL of the 10 mM $HAuCl_4$ were used up after about 600 s of electrodeposition. This was supported by the visual observation of the droplet turning clear (previously bright yellow) after the electrodeposition process. The absorbance mode of the surface was taken with respect to the SPCE chips to see the LSPR absorbance of the chip and the spectra showed an increasing absorbance at about 545 nm with increasing deposition time (Fig. S1). However, optimization studies would be required in future experiments, while this report will only focus on the reflectance property of the electrodeposited surface investigated under scope mode.

The growth of Au nanostructures on nucleation points was reported to form dendritic structures with thorns and branches [3]. In our observations, there were also obvious clusters formed as seen from the SEM images (Fig. S2). This was due to the tendency of the Au nanostructures forming clusters. Every layer of Au nanostructures assembled from nucleation points provided by nanostructures in the previous layer [15]. Leaf-like plate structures were also observed on these working electrodes. They seemed to have branching 'vein systems' just like those found in leaves. Characteristic dendritic structures could also be observed (Fig. S3). These structures provided evidence for the formation of a Au layer on our carbon working electrode. Observing a more layered structure in the 10,000× magnification of a 1000 s electrodeposition image as compared to the 700 s electrodeposition one, it may also be possible that the saturation of raw reflection signal was due to the almost complete coverage of the carbon electrodes at about 600 s and any further electrodeposition would only result in Au nanostructures forming on previously formed clusters, increasing the raw reflection signal insignificantly.

The raw reflection spectra and the electrodeposition time dependence of the peak intensities measured at 627 nm showed an increasing trend with the increasing deposition time (Fig. 2).

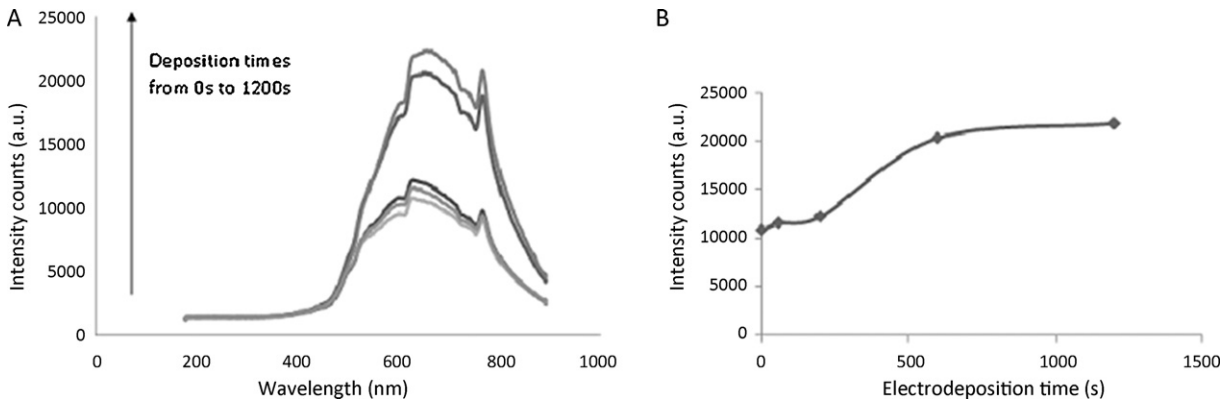

Fig. 2. Optical characterization of SPCEs after electrodeposition. (A) Raw reflection spectra taken in scope mode of the working electrode area of the Au deposited chips with increasing intensities from deposition times of 0 s, 60 s, 200 s, 600 s and 1200 s. (B) Deposition time dependence of peak intensity of raw reflection spectra at 627 nm.

The SEM images of the surface were in agreement with the ones reported by Chikae and co-workers [1]. The Au nanostructures deposited coated the working electrode surface uniformly for the 200 s deposition time, but formed large clusters after 600 s of electrodeposition (Fig. 3). This was attributed to the nucleation effect discussed earlier.

The stability of the gold electrodeposited structures were tested by measuring the reflectance intensity of the chips after a week and was found to be fairly consistent with fluctuations less than 5% of the original value after storage in a petri-dish at room temperature for a week. To evaluate the efficiency of deposition, we performed cyclic voltammetry and impedance spectroscopy. The deposition time used was chosen to be the duration where the surface is saturated with gold according to the optical spectra shown previously: 600 s for SPCEs. It was observed from impedance spectroscopy that the charge transfer resistance (CTR) decreased for SPCE chips (Fig. S4). However, the magnitude of decrease in CTR was significantly different. Nyquist plots were fitted by a simulated Randles equivalent circuit and the errors were calculated by the FRA software. These gold nanoparticles that were highly electrically conductive reduced the CTR of the working electrodes on chips. The cyclic voltammetry supported the impedance data, as well (Fig. S5). It could be seen that the integrated area of the cyclic voltammograms after electrodeposition was greatly increased. This supported the hypothesis that the electroactivity of the chips was tremendously increased after gold electrodeposition.

Instead of characterizing the electrodeposition of Au nanostructures on carbon surfaces with cyclic voltammetry, which would take up a few minutes for each measurement, our characterization with the raw reflection data was much faster and the Au surface was not perturbed by the redox process. A plateau effect could be observed with the raw reflection peak intensities against the time of electrodeposition from 0 to 1200 s. Further electrodeposition was not performed as the increase in peak intensity from

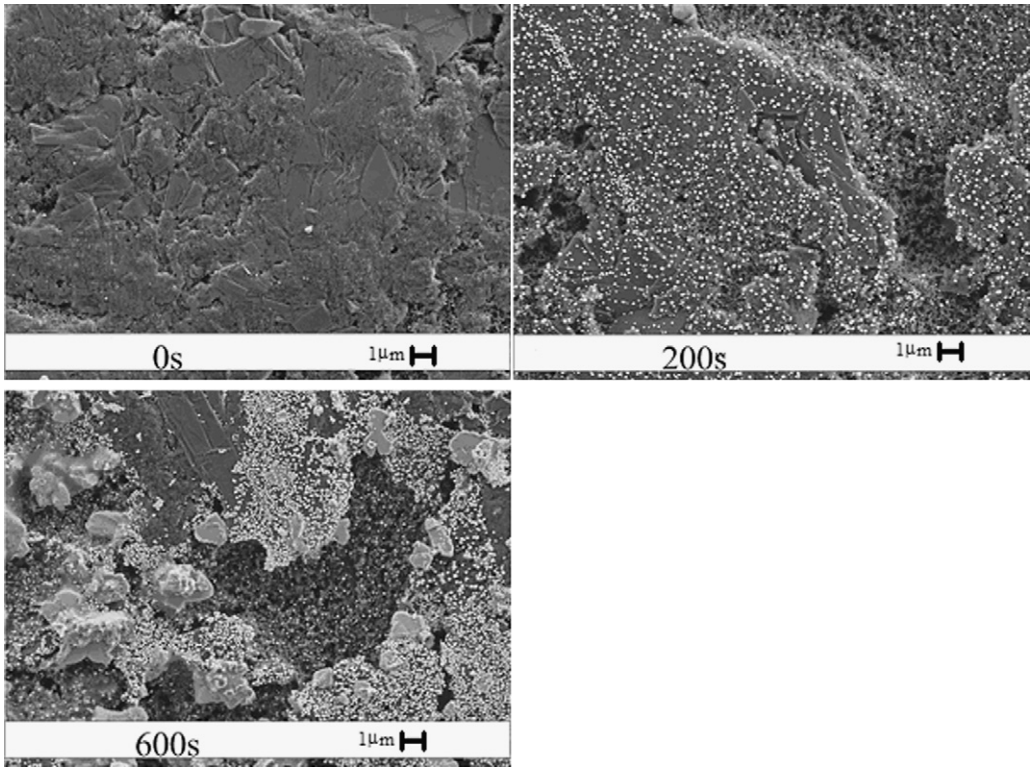

Fig. 3. SEM operated at 3.00 kV and using a working distance between 5 and 6 mm, images of electrodeposition of gold nanoparticles on SPCEs were produced at 5000× magnification. (A) Blank carbon surface of working electrode. (B) 200 s electrodeposition of gold nanoparticles. (C) 600 s electrodeposition of gold nanoparticles.

600 s to 1200 s was not significant and seemed to have saturated. A shorter electrodeposition time could be expected by increasing the $HAuCl_4$ concentration.

4. Conclusions

In conclusion, we have come up with a non-destructive optical confirmation of Au nanostructure formation on carbon surfaces of the SPCE chips. Such direct fabrication of metal nanostructures is simple and fast. Further optical characterization will be performed for biosensing experiments on these surfaces. Confirmation with electrochemical results will also be convenient as these chips are readily designed for such measurements. Au nanostructures on carbon chips provide a promising "dual-detection" platform for taking electrochemical and optical measurements on a single surface.

Acknowledgements

Authors gratefully acknowledge the financial support from the Alzheimer Society of Canada and NSERC Discovery Grant.

Appendix A. Supplementary data

Supplementary data associated with this article can be found, in the online version, at doi:10.1016/j.talanta.2011.08.039.

References

[1] M. Chikae, K. Idegami, K. Kerman, N. Nagatani, M. Ishikawa, Y. Takamura, E. Tamiya, Electrochem. Commun. 8 (2006) 1375–1380.
[2] F. Gao, M.S. El-Deab, T. Okajima, T. Ohsaka, J. Electrochem. Soc. 152 (2005) A1226–A1232.
[3] N. Sakai, Y. Fujiwara, M. Arai, K. Yu, T. Tatsuma, J. Electroanal. Chem. 628 (2009) 7–15.
[4] T.S. Olson, P. Atanassov, D.A. Brevnov, J. Phys. Chem. B 109 (2004) 1243–1250.
[5] C. Batchelor-McAuley, C.E. Banks, A.O. Simm, T.G. Jones, R.G. Compton, Analyst 131 (2006) 106–110.
[6] M.S. El-Deab, T. Okajima, T. Ohsaka, J. Electrochem. Soc. 150 (2005) A851–A857.
[7] V. Carralero, M.L. Mena, A. Gonzalez-Cortés, P. Yáñez-Sedeño, J.M. Pingarrón, Biosens. Bioelectron. 22 (2006) 730–736.
[8] H.M. Hiep, T. Endo, M. Saito, M. Chikae, D.K. Kim, S. Yamamura, Y. Takamura, E. Tamiya, Anal. Chem. 80 (2008) 1859–1864.
[9] N. Nath, A. Chilkoti, Anal. Chem. 74 (2002) 504–509.
[10] N. Nath, A. Chilkoti, Anal. Chem. 76 (2004) 5370–5378.
[11] T. Endo, K. Kerman, N. Nagatani, T. Yuzuru, E. Tamiya, Anal. Chem. 77 (2005) 6976–6984.
[12] T. Endo, S. Yamamura, N. Nagatani, Y. Morita, Y. Takamura, E. Tamiya, Sci. Technol. Adv. Mater. 6 (2005) 491–500.
[13] T. Endo, K. Kerman, N. Nagatani, H.M. Hiep, D.K. Kim, Y. Yonezawa, K. Nakano, E. Tamiya, Anal. Chem. 78 (2006) 6465–6475.
[14] K.M. Mayer, S. Lee, H. Liao, B.C. Rosto, A. Fuentes, P.T. Scully, C.L. Nehl, J.H. Hafner, ACS Nano 2 (2008) 687–692.
[15] J.B. Shein, L.M.H. Lai, P.K. Eggers, M.N. Paddon-Row, J.J. Gooding, Langmuir 25 (2009) 11121–11128.